Primary Research

Genetic depletion of Polo-like kinase 1 leads to embryonic lethality due to mitotic aberrancies

Paulina Wachowicz[1)2)], *Gonzalo Fernández-Miranda*[1)3)], *Carlos Marugán*[1)], *Beatriz Escobar*[1)4)] *and Guillermo de Cárcer*[1)*]

Polo-like kinase 1 (PLK1) is a serine/threonine kinase that plays multiple and essential roles during the cell division cycle. Its inhibition in cultured cells leads to severe mitotic aberrancies and cell death. Whereas previous reports suggested that Plk1 depletion in mice leads to a non-mitotic arrest in early embryos, we show here that the bi-allelic *Plk1* depletion in mice certainly results in embryonic lethality due to extensive mitotic aberrations at the morula stage, including multi- and mono-polar spindles, impaired chromosome segregation and cytokinesis failure. In addition, the conditional depletion of Plk1 during mid-gestation leads also to severe mitotic aberrancies. Our data also confirms that Plk1 is completely dispensable for mitotic entry in vivo. On the other hand, Plk1 haploinsufficient mice are viable, and Plk1-heterozygous fibroblasts do not harbor any cell cycle alterations. Plk1 is overexpressed in many human tumors, suggesting a therapeutic benefit of inhibiting Plk1, and specific small-molecule inhibitors for this kinase are now being evaluated in clinical trials. Therefore, the different Plk1 mouse models here presented are a valuable tool to reexamine the relevance of the mitotic kinase Plk1 during mammalian development and animal physiology.

Keywords:
cell cycle; development; mitosis; Polo-like kinase 1; spindle dynamics.

DOI: 10.1002/bies.201670908

[1)] Spanish National Cancer Research Centre (CNIO), Madrid, Spain
[2)] Ecole polytechnique fédérale de Lausanne (EPFL), Lausanne, Switzerland
[3)] Institute for Research in Biomedicine (IRB), Barcelona, Spain
[4)] Spanish National Cardiovascular Research Centre (CNIC), Madrid, Spain

*Corresponding author:
Guillermo. de Cárcer
E-mail: gcarcer@cnio.es

Received 8 May 2015; accepted 21 July 2015 (Originally published as DOI: 10.1002/icl3.1022)

Introduction

Polo-like kinase 1 (Plk1) was discovered, among many other cell cycle genes, in the 1980s from genetic screens performed in yeast and *Drosophila* [1–3]. Subsequently, Plk1 was revealed as a kinase very well conserved through evolution, from yeast (Cdc5 in *Saccharomyces Cerevisae*) to insects (Polo in *D. melanogaster*), amphibians (Plx1 in *Xenopus laevis*) and mammals (Plk1 in *Homo sapiens*) [4–9]. In the following years, the Polo-like kinase family expanded, and four members were added (Plk1, Plk3, Plk4 and very recently Plk5) [10–12]

Polo-like kinase 1 is a master regulator of cell division, controlling several important processes throughout the cell cycle, such as centrosome maturation [13], Golgi breakdown [14–17], spindle assembly [18–21], chromosome segregation [20,22,23] and cytokinesis [24–30]. All these processes are regulated by Plk1 upon phosphorylation of many different substrates [31]. Plk1 is differentially localized in the cell depending on the cell cycle phase [10]. During interphase, Plk1 is located at the cytoplasm and centrosomes. At the mitotic onset, when the nuclear envelope breaks down, Plk1 is highly concentrated at the migrating centrosomes and shuttles to the kinetochores of the condensed chromosomes. During chromosome separation at anaphase, Plk1 decorates the mitotic mid-zone, hence becoming concentrated at the mid-body where the two daughter cells will be separated.

Polo-like kinase 1 has a canonical kinase domain at the N-terminus. The regulatory domain, so-called the "polo-box domain" (PBD), is located at the C-terminus, and it confers the distinctiveness of the Polo-like kinase family [12,32,33]. The PBD is a unique structure that allows the recognition of proteins by a "pincer-like" 3D structure [34–36]. The mechanism by which Plk1 binds to its substrates is mainly based on the recognition of residues previously phosphorylated by other kinases [35,37]. Once Plk1 and the substrate are bound together, Plk1 can phosphorylate the substrate at neighboring residues. The recognition site is mostly based on the consensus sequence Ser-[pSer/pThr]-[Pro/X] [35]. Although this "phospho-priming" mechanism is the most common way for Plk1 to find substrates, there are also formal demonstrations that the Plk1 can bind substrates regardless of their phosphorylation status [36,38].

Polo-like kinase 1 inactivation in somatic cells, either by means of small-interference RNA or by chemical inhibition,

Bioessays **38**: S96–S106,

leads to spindle aberrations and problems in chromosome segregation and eventually to cell death due to a prolonged mitotic arrest [39–41]. In addition, Plk1 genetic depletion during animal development also promotes similar mitotic phenotypes and consequently animal death. Mutant alleles of *polo*, the *Drosophila* orthologue, leads to monopolar spindles in larval neuroblasts [2], and a hypomorphic *polo* allele shows cytokinesis failure in spermatocytes [42,43]. Similarly, depletion of the Plk1 yeast orthologues (*Cdc5* in budding yeast, or *plo1* in fision yeast) leads to proliferation arrest due to division alterations [44].

In mammals, Plk1 is expressed mainly in proliferating tissues [45,46]. In addition, this kinase is frequently found overexpressed in many tumors, and this feature often correlates with poor prognosis [47,48]. Consequently, Plk1 is currently considered a bona fide cancer therapeutic target. There is a growing collection of small compounds that are able to inhibit the kinase activity of Plk1 with high specificity. Several of these inhibitors are currently tested in chemotherapy clinical trials for different cancer types [49–52]. Therefore, any data resulting from Plk1 depletion in a mammalian model are of high value in the evaluation of Plk1 kinase as an anticancer therapeutic target.

In recent years, two mouse strains with genetically altered expression of Plk1 were reported. In 2008, Junjie Chen and colleagues described that embryos homozygous for a Plk1 gene-trap allele did not show any mitotic alterations. Surprisingly, cells appear to be arrested during interphase [53]. The other mouse model, reported in 2011 [54], is an inducible knock-down of Plk1 by inserting a short-hairpin RNA (shRNA) in the murine Rosa26 locus. This depletion strategy is conditional, allowing depletion in the adult animal. However, because depletion is driven by shRNA, it is difficult to evaluate the effects of full Plk1 depletion in this model, and embryonic development was not studied.

To clarify the effects of Plk1 depletion during embryonic development, we have generated a gene-trap allele, targeting intron 2 of the mouse *Plk1* locus. Our data confirms that Plk1 is an essential gene in mammals and Plk1-null mice die at the morula stage of embryo development due to severe mitotic aberrancies. Interestingly, Plk1 haploinsufficiency is fully compatible with animal life and *Plk1*(+/−) animals develop normally, as shown in previous reports [53]. We have also generated a conditional knock-out mice, to allow Plk1 depletion after embryonic mid-gestation. Conditional depletion of Plk1 at embryonic day E12.5 also leads to mitotic aberrations. Concomitantly, mouse embryonic fibroblasts (MEFs) derived from the *Plk1*(+/−) animals do proliferate with similar kinetics as their wild-type littermates and do not show any alteration in the cell cycle, whereas MEFs fully depleted of Plk1 show all the classical mitotic alterations already described. Thus, here we show that Plk1 is essential for the mammalian embryonic development, and its depletion leads to mitotic alterations and lethality at different stages during mammalian development.

Results

Plk1-deficient embryos show high levels of mitotic aberrancies

We have generated a *Plk1*(+/−) mutant mouse by using homologous recombination in Embryonic Stem (ES) cells with a specific insertion of a β-geo cassette into intron 2 of the mouse *Plk1* locus (Fig. 1A). No viable *Plk1*(−/−) mice were born from crosses between *Plk1*(+/−) heterozygous mice, and homozygous embryos were not found at any stage after implantation (E8.5) (Fig. 1B). We then tested the viability of the Plk1 null embryos at day E1.5 by isolating them immediately after fertilization and tracking their development in an in vitro culture. As depicted in Fig. 1C, both *Plk1*(+/+) and *Plk1*(+/−) embryos develop well in vitro during 4 days, reaching a morula like stage. The insertion of the β-geo cassette was verified by PCR (Fig. 1D), and the Plk1 expression during these initial stages was monitored by β-galactosidase staining activity (Fig. 1E), as well as immunofluorescence with Plk1-specific antibodies (Fig. 2B and C). *Plk1*(−/−) mutant embryos arrest at the morula stage by E3.5 and do not progress to form proper blastocysts (Figs 1C and 2A). Whereas *Plk1*(+/+) embryos show the typical Plk1 localization at the spindle poles in mitotic metaphase cells (Fig. 2B – solid arrow heads), and also at the mid-body and the cytokinetic furrow in anaphase cells (Fig. 2B – thin arrows), the *Plk1*(−/−) blastocytes do not show any positive staining for Plk1 (Fig. 2C – solid arrow heads pointing out the spindle poles), even though they present a high ratio of mitotic cells (42.2% in average).

A detailed immunofluorescence microscopic analysis shows that mitotic cells in the *Plk1*(+/+) embryos show symmetric bipolar spindles, with chromosomes properly arranged in the metaphase plate (Figs. 2B and 3A). In anaphase and telophase cells, sister chromatids seem to be equally segregated to each daughter cell (Fig. 2B). In contrast, Plk1 null embryos displayed a substantial arrest of cells in a prometaphase-like stage (42.2% in average), with incomplete metaphase plates and misaligned chromosomes (Fig. 3B). Additionally, no anaphase and telophase figures were observed, confirming the impairment of chromosome segregation. Most of the mitotic arrested cells, in the Plk1 null embryos, displayed monopolar (34.7% in average) or multipolar spindles (13.0% in average) with poorly focused spindle poles (52.3% in average). Consequently, cells also showed misaligned chromosomes (Fig. 3B – arrow heads), thus confirming the role for Plk1 in the establishment of bipolar spindles and proper chromosome alignment also during the embryonic development. Interestingly, few Plk1 null cells showed enlarged nucleus with an increased number of centromeres (as depicted by anti-centromere antibody (ACA) staining) when compared with *Plk1*(+/+) embryos or even the neighboring cells in the same blastocyst (Fig. 3C – arrow). These cells most likely progress through mitosis and, as a consequence of cytokinesis defects, form polyploid cells. These cytokinesis alterations might also explain the higher incidence of multipolar spindles we observed, as polyploid cells probably enter in the following round of division with an extra number of centrosomes. All these cellular defects eventually can lead to cell death, thus explaining the *Plk1*(−/−) embryo lethality by E3.5–E5.5.

Plk1 haploinsufficient MEFs do not show any cell cycle alteration

Because Plk1 haploinsufficient animals were born and develop normally, we were able to obtain MEFs from *Plk1*(+/−) E13.5

A)

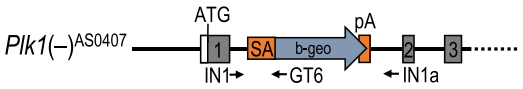

B)

Developmental Stage	Total	*Plk1(+/+)*	*Plk1(+/–)*	*Plk1(–/–)*
Born	232	90 (39%)	142 (61%)	0 (0%)
Mid-gestation (E8.5-E10.5)	22	7 (32%)	15 (68%)	0 (0%)
Two cell stage (E1.5)	108	34 (31%)	47 (44%)	27 (25%)
	Expected %	(25%)	(50%)	(25%)

C)

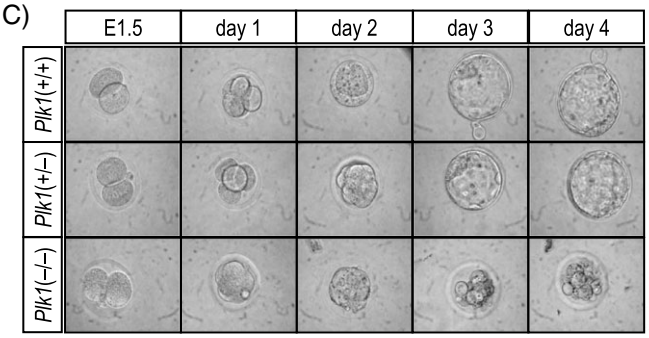

D)

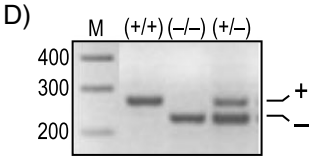

E)

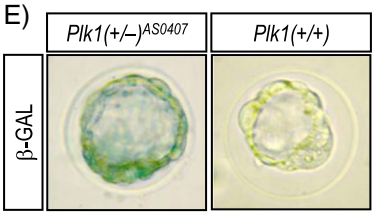

Figure 1. Early embryonic lethality of the Polo-like kinase 1 (Plk1) null mice. **A**: Scheme of the Plk1 gene-trap AS0407. A splicing acceptor sequence (SA) fused to a beta-geo (b-geo) cassette, and followed by a poly-adenilation signal (pA), are inserted into intron 2 of the *Plk1* murine locus. **B**: Table showing the offspring Mendelian statistics of the $Plk1^{AS0407}$ strain. There are no *Plk1*(–/–) born animals, neither mid-gestation embryos (E8.5–10.5). When embryos are genotyped at E1.5 post-coitum, we find the adequate Mendelian ratio of each genotype. **C**: Post-coitum embryos are extracted from crosses between *Plk1*(+/–) animals. E1.5 embryos are cultured in vitro and followed in a daily time course under the microscope. Whereas *Plk1*(+/+) and *Plk1*(+/–) progress normally to the blastocyst stage, *Plk1*(–/–) embryos arrest at the morula stage by E3.5 and undergo apoptosis. **D**: After 4 days of culture, DNA is extracted from cultured embryos and subjected to PCR using specific oligonucleotides, in order to evaluate the insertion of the b-GEO cassette into the *Plk1* locus, and determine the genotype regarding the gene trapping. **E**: *Plk1*(+/–) blastocysts express the beta-gal cassette and can be stained for beta-galactosidase in order to verify the expression of the transgene, whereas the *Plk1*(+/+) that do not harbor the b-GAL cassette remain stainless.

embryos. When compared with littermates *Plk1*(+/+) MEFs, *Plk1*(+/–) expresses half the levels of Plk1 protein in both proliferating and arresting cultures (Fig. 4A). *Plk1*(+/–) cells did not display any alteration in their cell cycle profile, showing similar percentages within all cell cycle phases as depicted by DNA content via flow cytometry (Fig.4B). Additionally, *Plk1*(+/+) and *Plk1*(+/–) MEFs showed similar proliferation rates (Fig. 4C). This is consistent with the in vivo data where E16.5 heterozygous embryos showed similar levels of BrdU incorporation rates as their wild-type littermates (Fig. 4D). Finally, despite the reduction on Plk1 levels in the heterozygous MEFs, these cells did not show any significant change in ploidy when compared with *Plk1*(+/+) MEFs (Fig. 4E). Altogether, these data demonstrate that Plk1 haploinsufficiency is compatible with a normal cell cycle progression and proliferation rate.

Conditional depletion of Plk1 leads to mitotic arrest and cell death

In order to confirm that full depletion of Plk1 leads to mitotic arrest and cell death, we have also generated a conditional depletion model for Plk1, by using the CAG-Flpe transgenic strategy [55]. Two lox-P sites were inserted flanking the Plk1 exon 2 by homologous recombination in ES cells, generating the *Plk1*(lox)

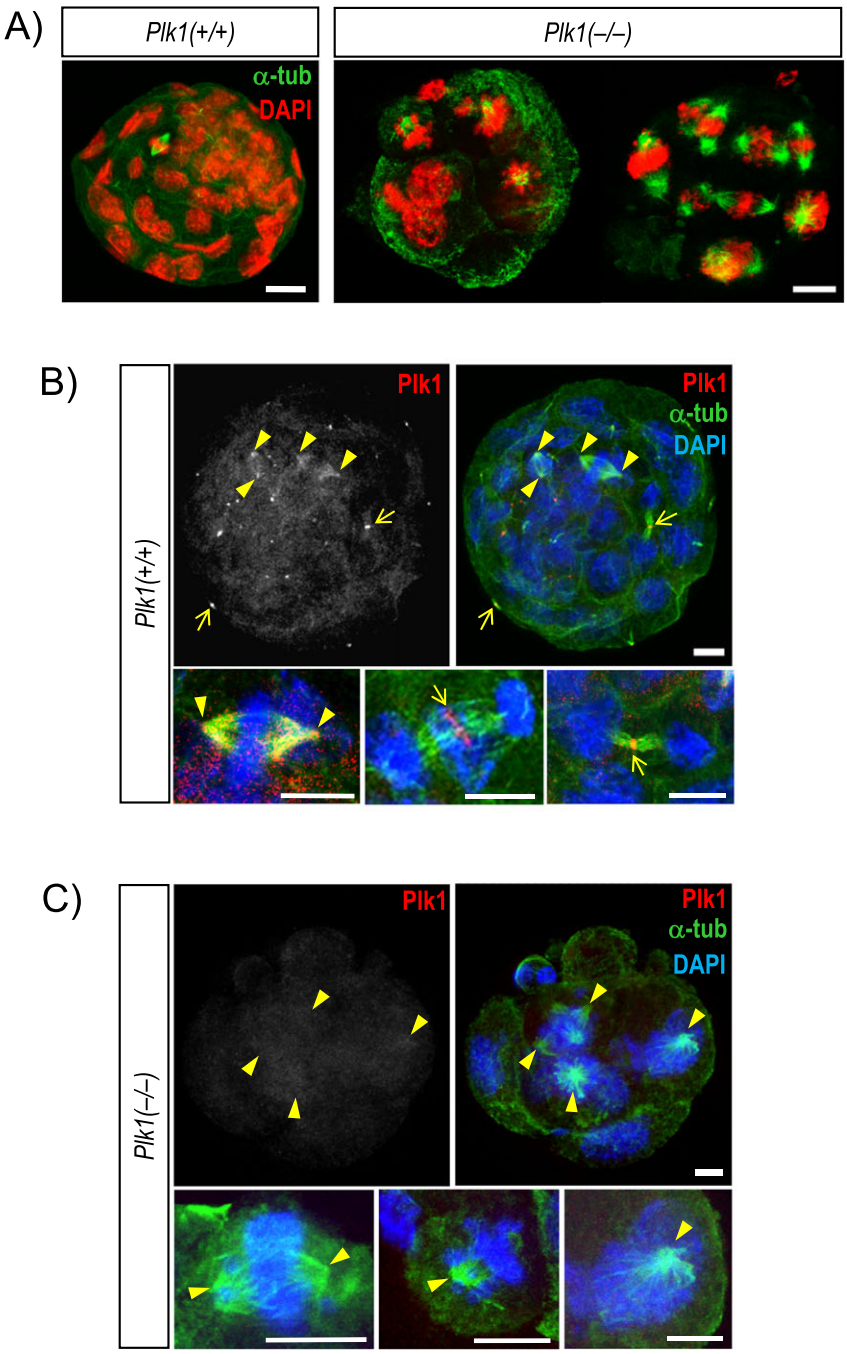

Figure 2. Mitotic arrest in the Polo-like kinase 1 (Plk1) null embryos. **A**: Immunoflorescence analysis of *Plk1*(+/+) *and Plk1*(−/−) embryos. By E3.5., *Plk1*(+/+) embryos (left panel) show few mitotic cells with a normal-shaped spindle, as detected by immunostaining of α-tubulin (green) and counterstained DNA (red). Plk1 null embryos (right panel) arrest in a 10–12 cell morula stage with most cells arrested in an aberrant mitosis. Bar indicates 10 μM. **B**: *Plk1*(+/+) embryos display a precise Plk1 staining (red) at the mitotic spindles poles (arrowheads), anaphase mid-zone and the cleavage furrow at cytokinesis (arrow). Tubulin is stained in green and DNA counterstained in blue. Bar indicates 10 μM. **C**: *Plk1*(−/−) embryos do not show any Plk1 staining (red) although most of the cells are arrested in mitosis as shown by tubulin staining (green). Arrow heads indicate the aberrant mitotic spindle poles. DNA is counterstained in blue. Bar indicates 10 μM

locus (Fig. 5A). MEFs extracted from *Plk1*(lox/lox) E13.5 embryos proliferate normally, showing no differences when compared with *Plk1*(+/+) control cells (data not shown). In order to deplete Plk1 completely, *Plk1*(lox/lox) MEFs were synchronized by serum starvation and infected with Adeno-CRE virus facilitating loci excision. Plk1 depletion efficiency was verified by PCR (Fig. 5B) and by immunoblotting (Fig. 5C).

To analyze cell cycle progression in the absence of Plk1, *Plk1*(*lox*/*lox*) MEFs were synchronized in Go by serum starvation, infected with Adeno-Cre viruses and then released in

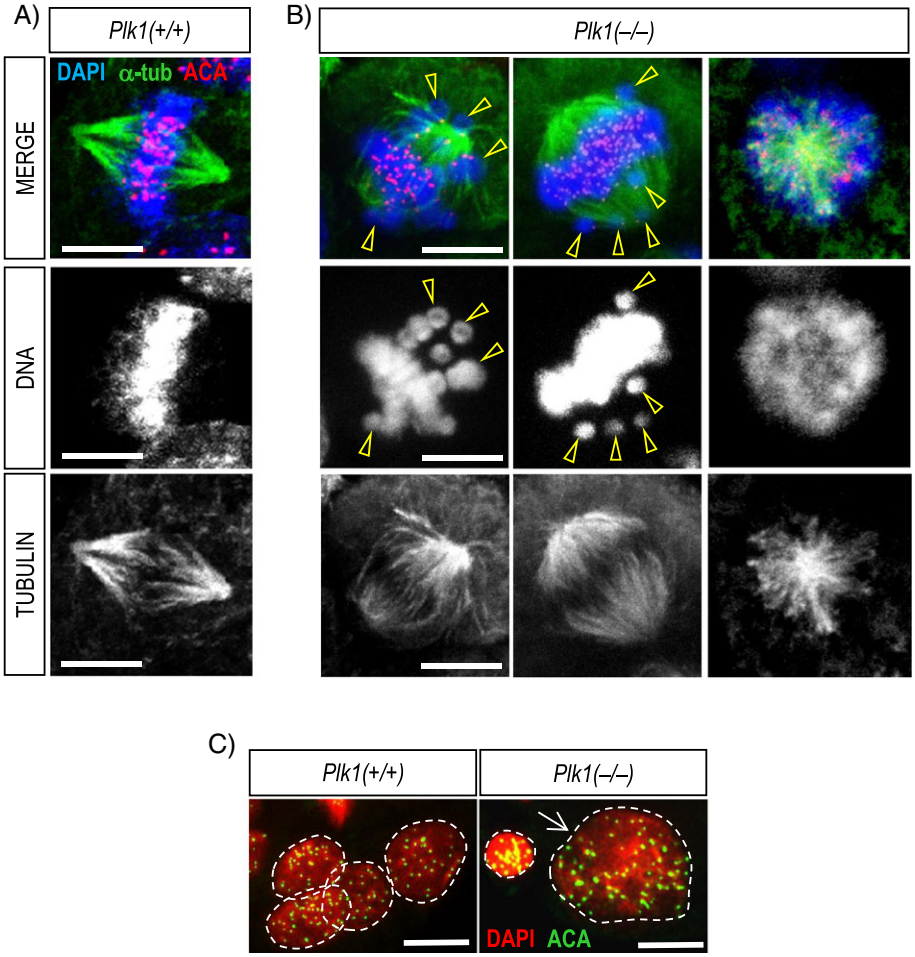

Figure 3. Mitotic aberrations in the Polo-like kinase 1 (Plk1) null embryos. **A**: Wild type embryos contain canonical metaphases with properly aligned chromosomes and bipolar spindles as shown by staining with α-tubulin (green), anti-centromere antibody (ACA) signal at the centromeres (red) and counterstained DNA (blue). Bar represents 10 μm distances. **B**: Detailed mitotic pictures from *Plk1*(−/−) E3.5 embryos displaying severe spindle aberrancies, with unfocused spindle poles and monopolar spindles, all accompanied with a high number of misaligned chromosomes (open arrow heads). Bar represents 10 μm distances. **C**: The presence of giant cells (arrow) with decondensed chromosomes in the *Plk1*(−/−) embryos suggest a defect in cytokinesis in the absence of Plk1 (right panel). These polyploid cells present around 80 ACA-stained spots (green) whereas most the other cells in the same embryo, or in *Plk1*(+/+) embryos have about 40 ACA spots. Bar represents 10 μm distances.

high-serum media and followed in a time course (Fig. 5D). *Plk1*(Δ/Δ) cells enter into the cell cycle and go through G1, S and G2 phases with no evident restrictions (Fig. 5E). However, 36 hours post-release in high-serum media, *Plk1*(Δ/Δ) MEFs showed an arrest in the mitotic phase, as measured by MPM2 staining, in contrast to *Plk1*(*lox*/*lox*) cells. Concomitantly, the cell cycle DNA content profile shifts towards the G2/M peak (Fig. 5F). Microscope examination of arrested cells revealed all the typical mitotic aberrancies due to Plk1 inhibition, such as monopolar and multipolar spindles, non-aligned chromosomes and lagging chromosomes (Fig. 5G and H).

We then wanted to extrapolate these in vitro data into the mouse embryo, to verify that Plk1 is also essential during post-implantation embryonic development. Plk1 is ubiquitously expressed in the E14.5 mouse embryo as detected by immunohistochemical analysis (Fig. 6A). There are specific areas where Plk1 expression is higher such as the developing neuroepithelia, the fetal liver, intestines and other epithelial structures. Plk1 is highly expressed in the mitotic cells along the embryo, nicely decorating the spindle poles and the mid-body of the mitotic cells (Fig. 6B).

To test the effects of Plk1 depletion during mid-gestation, *Plk1*(+/lox) female mice were crossed with *Plk1*(+/lox) male mice. At E12.5 day post-coitum, tamoxifen citrate salt (0.3 mg per gram of animal body weight) was intraperitoneally injected into the pregnant females and the embryos were collected for histology 2 days after tamoxifen injection, at day E14.5. Although changes in the embryo size were not detected, a detailed inspection of the proliferative areas such as the neuroepithelia showed that Plk1 depletion impairs mitosis. Whereas the *Plk1*(+/Δ) embryos displayed a normal distribution of mitotic cells in the neuroepithelia (Fig. 6C – open arrows), the *Plk1*(Δ/Δ) embryos showed an increase in aberrant mitotic figures, with evident alterations in chromosome alignment (Fig. 6C – closed arrows). There was an associated increase in the mitotic cell population, as depicted by

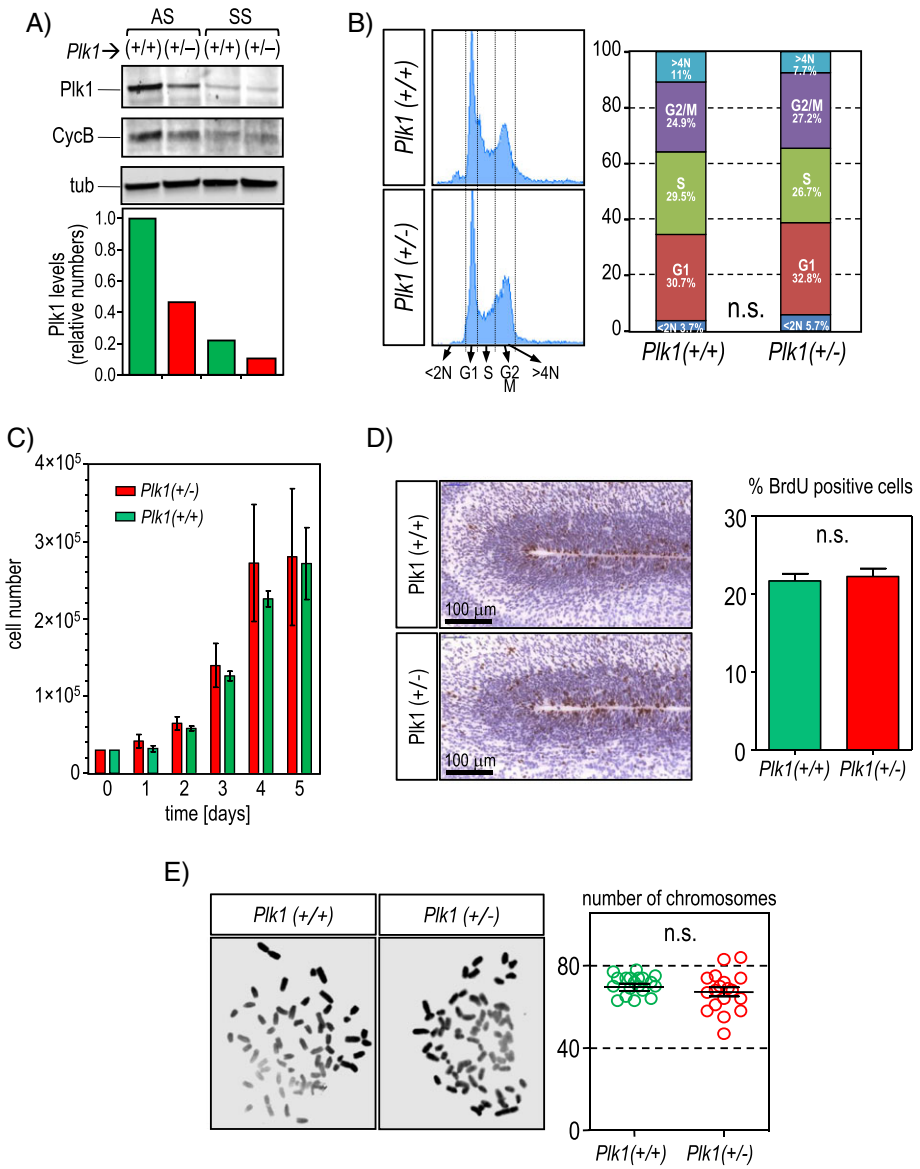

Figure 4. Polo-like kinase 1 (Plk1) haploinsuffcient mouse embryonic fibroblasts (MEFs) do not show cell cycle alterations. **A**: Plk1 expression analysis in MEFs from *Plk1*(+/–) and wild-type littermates. Asynchronic (AS) or serum starved (SS) cells were subjected to immunoblot for Plk1 detection, showing a clear reduction in Plk1 levels when compared with the *Plk1*(+/+) cells. Alpha-tubulin is used as a loading control, and Cyclin B as a read-out of the serum starvation. Histogram represents Plk1 protein quantification normalized versus the tubulin signal. **B**: DNA content profile, using propidium iodide, of immortal *Plk1*(+/+) and *Plk1*(+/–) MEFs showing no differences in the distribution of the different cell cycle phases. **C**: Proliferation curve of MEFs derived from *Plk1*(+/+) and *Plk1*(+/–) embryos. Both cell populations grow with similar kinetics. **D**: BrdU incorporation and quantification in the SVZ area of brains from *Plk1*(+/+) and *Plk1*(+/–) E16.5 embryos. Proliferation index in both genotypes are similar ($N \geq 3$ embryos per genotype). **E**: Karyotyping of immortal *Plk1*(+/+) and *Plk1*(+/–) MEFs showing no major differences in chromosome number.

phospho-Ser10 Histone H3 immunostaining (Fig. 6D – upper panel). The Plk1 depletion was confirmed in the aberrant mitotic cells by the absence of Plk1 staining (Fig. 6D – lower panel, closed arrows). Interestingly, similar phenotypes could be observed in other proliferating tissues such as the fetal liver (data not shown).

Altogether, our data confirm that Plk1 is essential during embryonic development at several stages, and Plk1 depletion during the mouse embryonic development leads to severe mitotic aberrancies such as multipolar and monopolar spindles, lagging chromosomes and cytokinesis failures.

Discussion

From yeast to mammals, Plk1 is one of the crucial mitotic regulators. In addition, Plk1 is a relevant molecule in the cancer clinics because it is highly expressed in many tumors, it is a poor prognostic marker and, more importantly, it is considered as a relevant therapeutic target. There are several small-molecule inhibitors for Plk1 already in clinical trials for cancer therapy [50]. In this context, any relevant information of the physiological changes generated by Plk1 inhibition in mammals is important as a validation strategy for these inhibitors.

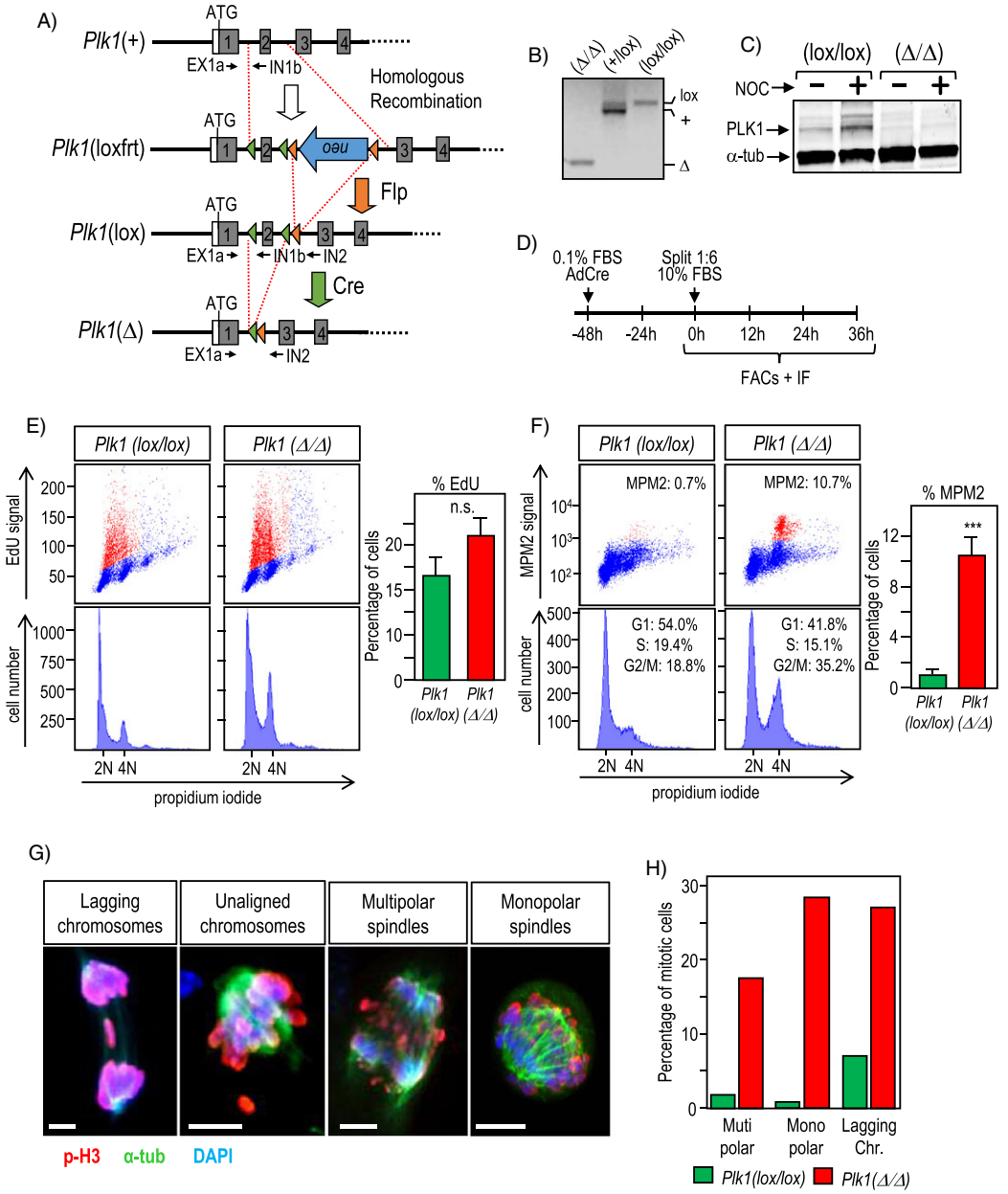

Figure 5. Conditional Polo-like kinase 1 (Plk1) depletion in mouse embryonic fibroblasts (MEFs) upon Cre expression. **A**: Scheme of the Plk1 conditional knock-out strategy. By homologous recombination, the *Plk1* exon 2 is flanked with lox-P (green triangles) and Frt (orange triangles) recombination sequences and a neomycin phosphotransferase cassette (NEO) generating the *Plk1*(frtlox) locus. Upon expression of the Flip recombinase, the NEO cassette is excised from the Frt sites, generating the *Plk1*(lox) allele. Finally, when Cre recombinase is expressed, exon 2 is removed from the Lox-P sites leading to a DNA frame shift that generates the null allele *Plk1*(Δ). **B**: Plk1 depletion validation by PCR using specific oligonucleotides to detect the depleted (Δ/Δ) and the non-depleted (lox/lox) locus. **C**: Western blot to validate Plk1 absence in the *Plk1*(Δ/Δ) cells. Nocodazole (NOC) was added to the cells during 16 hours in order to arrest cells in mitosis and detect the maximum peak of Plk1 expression. α-tubulin is used as a loading control. **D**: Flow chart of the synchronization protocol for MEFs and Adeno-Cre infection. Full confluent and serum starved *Plk1*(lox/lox) cells are infected with either AdCre or AdGFP viral particles during 48 hours. Then, cells are seeded at one-sixth dilution in 10% serum media, and time points are taken each 12 hours. **E**: EdU incorporation FACs analysis 36 hours after entering the cell cycle. *Plk1*(Δ/Δ) cells are able to enter the cell cycle when recovered from the serum starvation arrest. *Plk1*(Δ/Δ) cells undergo G1 and S phases with similar kinetics as the *Plk1*(lox/lox) control cells, as quantified in the right histogram. **F**: FACs analysis 36 hours after entering into the cell cycle. *Plk1*(Δ/Δ) cells show an increase in the mitotic index when compared with *Plk1*(lox/lox) as depicted by the staining with the mitotic marker MPM2 (upper panels) and quantification histogram. DNA content analysis, using propidium iodide staining, shows an increase in the G2/M population of the *Plk1*(Δ/Δ) cells. **G**: Mitotic aberrancies upon Plk1 depletion. *Plk1*(Δ/Δ) MEFs were subjected to immunofluorescence for alpha-tubulin (α-tub – green) and phospho-Ser10 Histone H3 (pH3 – red) and DNA counterstained with DAPI (blue). Cells show all the classical phenotypes of Plk1 inhibition such as monopolar and multipolar spindles, and unaligned or lagging chromosomes. **H**: Quantification histogram of the different mitotic fates when comparing control *Plk1*(lox/lox) cells versus *Plk1*(Δ/Δ) MEFs.

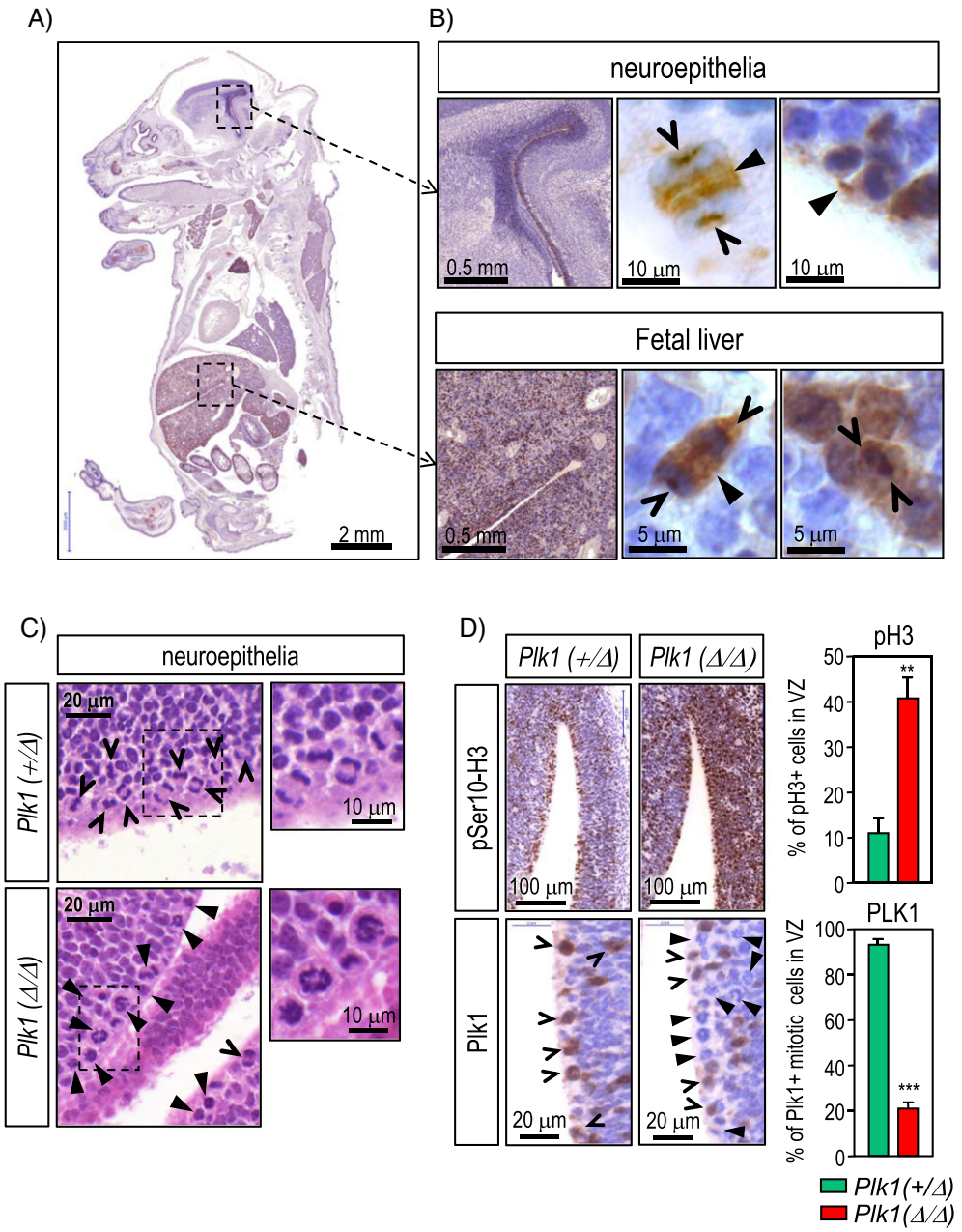

Figure 6. Polo-like kinase 1 (Plk1) depletion during embryonic mid-gestation leads to mitotic aberrancies. **A**: Plk1 expression analysis in E16.5 mouse embryos. Plk1 is widely express in the mouse embryo as depicted by immunohistochemistry using Plk1 antibody. **B**: Plk1 expression is higher in the most proliferative areas such as the embryonic neuroepithelia (upper panel) and the fetal liver (lower panel). Mitotic cells show the correct Plk1 subcellular distribution, with high staining at the spindle poles (open arrow) and the anaphase mid-zone (solid arrow). Bars show magnification in each microphotograph. **C**: Plk1 depletion leads to mitotic aberrancies in the embryonic neuroepithelia. E12.5 embryos were treated with tamoxifen, to activate Cre recombinase, and analyzed 48 hours later at day E14.5. Whereas the *Plk1*(+/Δ) embryos show normal pattern of cell division at the SVZ of the brain (upper panel – open arrows), the *Plk1*(Δ/Δ) littermates show an increase in aberrant mitotic figures in the brain neuroepithelia (lower panel – solid arrows). Insets show a higher magnification image of the mitotic cells. **D**: Immunohistochemistry of phosphoSer10-Histone H3 and Plk1 in the E14.5 embryonic brains from panel C. Plk1 depletion leads to a dramatic mitotic arrest in the SVZ area as depicted by pSer10-H3 staining and quantification (upper panels). Concomitantly, Plk1 depletion is verified by Plk1 staining (lower panels), where aberrant mitotic cells are devoid of Plk1 signal (solid arrows). Only a remnant of 20% of mitotic cells still have some levels of Plk1 expression in the *Plk1*(Δ/Δ), whereas almost 100% of the control mitotic cells are highly stained by the Plk1 antibody (lower panels). More than 500 cells were counted from three different embryos per genotype.

Complete genetic depletion of Plk1 leads to embryonic lethality at the morula stage. In the present study, the *Plk1*(−/−) morula cells recapitulate all the established phenotypes associated to Plk1 inhibition, from metaphases with misaligned chromosomes, to monopolar or multipolar spindles and even cytokinesis failure, as there are some interphase cells with double amount of

centromeres. A previous report by J. Chen and colleagues also showed that the constitutive genetic depletion of Plk1 leads to embryonic lethality at the morula stage [53]. Surprisingly, these Plk1-depleted embryos had no mitotic alterations, and cells are somehow arrested at an interphase stage. The possible discrepancies between the results observed in both reports might result from using different gene-trap strategies. J. Chen Plk1 knock-out mice were generated by using a gene-trap in intron 9 of the *Plk1* locus. Thus, there is still the chance of having a Plk1 protein expression in a truncated form only lacking the very C -terminal part of the protein and, therefore, still having some functionality. Another possible explanation for the non-mitotic phenotype is the fact that Plk1 was also described as an important driver for mitotic entry [56], thus, cells depleted in Plk1 would not be able to progress through G2 and stop before reaching mitosis. Although Plk1 participates in mitotic entry through phosphorylation of CDC25C, Myt1, Cyclin B and FoxM1 [57] and promotes recovery from DNA damage [58], it is not strictly required for mitotic entry [20,25,41]. The most probable explanation is that many of the proteins involved in the molecular network for mitotic entry are redundant in their function, as they play into several signaling feedback loops with no exclusive dependency in any of them. We validate that in our models all the cells are arrested at mitosis upon Plk1 depletion, either in the mice embryos or in vitro cell cultures, and there is no evidence of cell cycle stoppage before mitosis. All together, these data argue against an essential role for Plk1 in regulating mitotic entry and confirms an essential requirement for this protein during the formation of a functional bipolar spindle and chromosome segregation.

The predominant phenotype described when Plk1 is acutely chemically inhibited is the generation of monopolar spindles due to impartment of centrosome maturation and separation [41]. Interestingly, Plk1-depleted embryos not only display monopolar spindles but also multipolar spindles with unfocused poles. This circumstance probably comes from the fact that Plk1 depletion does not happen as efficiently as the chemical inhibition of the catalytic activity of Plk1. Thus, cells might be able to go through mitosis with a minimal residual of Plk1 but not have enough Plk1 levels to accomplish cytokinesis properly, as this seems to be one of the more demanding activities of Plk1 [24,30,59]. Consequently, cells would exit mitosis being polyploid, and they probably enter in the subsequent mitotic round with an extra number of centrosomes. Another explanation is the fact that Plk1 interplays with centrosomal proteins such as Kizuna, Aurora A or TPX2, and this might lead to multipolar spindles as well [60,61].

Polo-like kinase 1 null embryos are able to reach the morula stage with 12 to 16 cells. Thus, several rounds of cell division happened despite the Plk1 depletion. This is most probably due to maternal contribution, because Plk1 activity inhibition by specific drugs stops the very first mitotic division in the mouse embryo [62]. Similarly, Plk1 is essential for the mouse oocyte maturation, as it is critical for the oocyte meiotic resumption [63].

Polo-like kinase 1 needs to be entirely depleted or acutely inhibited in order to provoke aberrant mitosis. Meanwhile full depletion of Plk1 leads to severe mitotic aberrancies in embryo development and in MEFs in culture, *Plk1*(+/−) mice are viable and they follow the correct Mendelian ratio. In vitro, *Plk1*(+/−) MEFs do not show any alteration in their cell cycle profile and have identical proliferation index as the wild-type littermates derived cells (Fig. 4B and C). Thus, Plk1 haploinsufficiency does neither compromise cell viability nor cell cycle progression. Concomitantly, Klaus Strebhardt and colleagues engineered a mouse with an inducible Plk1-shRNA [54]. The shRNA used in this report is only able to reduce Plk1 levels up to 70% in mouse fibroblasts. These mice, even though they are able to reduce Plk1 levels very efficiently in certain tissues (86% in testis, 72% in bone marrow and 60% in spleen), silencing is not complete in some others (stomach or colon), and mice live with no major drawbacks with the remnant Plk1. Indeed, Plk1 knocked-down animals do not differ significantly from the wild-type counter littermates in terms of histology and metabolism. Accordingly, MEFs derived from these inducible knock-down mice tolerate Plk1 reduction up to 90%, with no alteration in cell proliferation. Plk1 being an essential kinase for cell proliferation and animal life, a minimal threshold of Plk1 expression or function is sufficient for cell progression and thereby an interesting observation given the current relevance of Plk1 as a putative cancer target.

Materials and Methods

Generation of Plk1 mutant mice

We generated *Plk1*(+/−) mutant mice by microinjection of the ES clone AS0407 (Sanger Gene Trap Resource; http://www.sanger.ac.uk/PostGenomics/genetrap/) into C57BL/6J blastocysts. These clones carry a β-geo (fusion between neomycin-resistant gene and β-galactosidase gene) cassette in the *Plk1* intron 2 (Fig. 1A). The position of the gene-trap cassette in these ES clones was confirmed by RT-PCR using the following primers: IN1_F (5′-AAGGCTTCTAGCGAGGGTACTTGGCACT-3′) and IN1a_R (5′-GCTAGGACTAGACGCTCGGAGTGGAGA-3′) both annealing in the murine *Plk1* intron 1 amplifying the wild-type allele and GT6_R (5′-GGGACAGTGCAGATCCAAAA–3′) annealing at the β-geo cassette to detect the trapped allele.

The Plk1 conditional targeting construct was assembled following the same strategy as previously reported in [64]. We flanked exon 2 of the murine *Plk1* locus with loxP sequences, thus generating the *Plk1*(lox) locus. A neomycin phosphotransferase (neo) cassette was used for positive selection of ES cell clones. Recombinant ES cells and clones were selected by southern blot. To conditionally generate a null allele *Plk1*(Δ), we crossed the *Plk1*(+/lox) mice with transgenic mice that express the Cre recombinase fused to the estrogen receptor (Cre-ERT2) inserted in the collagenase locus (Fig. 5A). All animals were maintained in a mixed 129/Sv (25%) times CD1 (25%) times C57BL/6J (50%) background. The following oligonucleotides for the Plk1 cKO genotyping were used: EX1a_F (5′-ACAGCGACTTTGTATTTGTAGTTTTG-3′) and IN1b_R (5′-CACTTTATGAATCCATTTCCTGTACC-3′) for detecting the wild-type and lox alleles and IN2_R (5′-TTTCAGCTTAGTAAAGAGACA-3′) for the depleted allele.

Histological and pathological analysis

Mice were housed at the pathogen-free animal facility of the Centro Nacional de Investigaciones Oncológicas (CNIO, Madrid) following the animal care standards of the institution. These animals were observed on a daily basis, and sick mice were humanely euthanized in accordance with the Guidelines for Humane End Points for Animals used in biomedical research. For histological observation, dissected organs were fixed in 10% buffered formalin (SIGMA-Aldrich St. Luis, MO, USA) and embedded in paraffin wax. Three- or five-micrometer-thick sections were stained with hematoxylin and eosin. Additional immunohistochemical examination of the tissues and pathologies analyzed was performed using specific antibodies against Plk1 (rat monoclonal – laboratory made), phospho-histone H3 Ser10 (Merck-Millipore, Billerica, MA, USA. 06-570) and anti-BrdU (GE Healthcare Buckinghamshire, UK RPN202).

Embryo cultures and immunofluorescence

Fertilized embryos were collected by flushing the uteri of pregnant females from crosses between *Plk1*(+/−) mice, with Hepes-buffered Medium 2 (M2; SIGMA-Aldrich St. Luis, MO, USA) at E1.5-E2.5. Embryos were individually cultured in vitro in potassium simplex optimized medium (KSOM; Chemicon International Inc., Billerica, MA, USA) and photographed daily for up to 5 days. For immunofluorescence analysis, embryos were fixed with cold methanol during 1 hour at −20 °C, rinsed with M2 medium, washed in phosphate buffered saline (PBS) containing 0.1% BSA (Sigma, St. Louis, MO, USA) and incubated with 0.1% Triton X. Embryos were then blocked with 10% of serum in PBS 0.1% BSA and incubated with the following primary antibodies: alpha-tubulin (DM1a, Sigma St. Louis, MO, USA), anti-centromere antibody (ACA, Antibodies Inc., Davis, CA, USA), PLK1 (Abcam ab14209, Cambridge, UK), and phospho-histone H3 Ser10 (06-570 Merck-Millipore, Billerica, MA, USA) for 2 hours at 37 °C. The matching secondary antibodies, with different Alexa dyes (488, 594, 647 or 680) are from Molecular Probes (Invitrogen Eugene, OR, USA). Images were obtained using a confocal ultra-spectral microscope (Leica TCS-SP5-AOBS-UV, Leica-Microsystems CMS GmbH, Mannheim, Germany).

To detect β-galactosidase activity, embryos were fixed for 5 minutes in PBS containing 1% formaldehyde, 0.2% glutaraldehyde and 1% serum. After fixation, embryos were rinsed with 1% serum in PBS and then transferred to a β-galactosidase reaction mixture (4 mM $K_3Fe(CN)_6$, 4 mM $K_4Fe(CN)_6$, 2 mM $MgCl_2$ and 1 mg/ml X-gal in PBS) at 37 °C overnight. Embryos were washed once in PBS and kept at 4 °C. Positive embryos were scored 48 hours after the reaction was initiated.

MEFs extraction, cell cycle profile and immunofluorescence

Mouse embryonic fibroblasts were prepared from E13.5 embryos and cultured using standard protocols [64]. Cell cycle profiling analysis was performed by detecting DNA content and EdU incorporation using the FACSCanto flow cytometry device (BD Biosciences Franklin Lakes, NJ, USA). EdU was added to exponential growing MEFs for 20 hours, and then cells were trypsinized and fixed in cold 70% ethanol. EdU staining protocol was performed following manufacture instructions (Click-iT, Invitrogen, Eugene, OR, USA), and DNA was stained with propidium iodide for 30 minutes. Mitotic index was determined by immunostaining with anti-MPM2 antibody (Millipore 05-368).

Immunofluorescence was performed by fixing the cells in 4% paraformaldehyde in PBS. After permeabilization with cold methanol, cells are blocked with 10% fetal bovine serum (FBS) in PBS and probed with specific antibodies against alpha-tubulin (DM1a, Sigma) and phospho-histone H3-Ser10 (Millipore 06-570). The secondary antibodies coupled to either Alexa488 or Alexa594 dyes are from Molecular Probes (Invitrogen). DNA is counterstained with DAPI, and cells are finally mounted in glass slides using Mowiol. Pictures were obtained using a confocal ultra-spectral microscope (Leica TCS-SP5-AOBS-UV).

Protein extraction and immunoblotting

For immunoblotting, MEFs were either asynchronous grown in 10% FBS (AS) or serum starved in 0.1% FBS for 48 hours (SS). Cells were then lysed in RIPA lysis buffer (37 mM NaCl, 0.5% NP-40, 0.1% SDS, 1% TX-100, 20 mM Tris–HCl pH 7.4, 2 mM EDTA, 10% glicerol 1 mM PMSF) and supplemented with protease and phosphatase inhibitory cocktails (SIGMA-Aldrich St. Luis, MO, USA). Proteins lysates were then separated in Criterion XT acrylamide gels (BioRad Hercules, CA, USA), transferred to nitrocellulose membranes (BioRad), probed using specific primary antibodies against PLK1 (Life Technologies 33-1700), cyclin B (Santa Cruz Biotechnology Dallas, TX, USA. sc-594) and α-tubulin (DM1a, Sigma) and detected using fluorescent secondary antibodies coupled to Alexa680 dye (Invitrogen) using the Odyssey Infrared Imaging System (Li-Cor Biotechnology, Lincoln, NE, USA).

Statistical analysis

Statistical analysis was performed using Student's *t*-test or analysis of variance (GraphPad Prism 5). All data are shown as mean ± SEM; probabilities of $p < 0.05$ were considered significant.

Acknowledgements

P. W. performed most of the cellular and mouse experiments, with technical support from G. F. M. B. E. and C. M. helped to perform biochemical experiments. G. d. C conceived the project and wrote the manuscript. P. W. received fellowships from the Marie Curie activities of the European Commission (Oncotrain programme). This article is funded by grants from the OncoCycle Programme (S2010/BMD-2470) from the Comunidad de Madrid and the European Union Seventh Framework Programme (MitoSys project; HEALTH-F5-2010-241548).

References

1. **Hartwell LH**, **Smith D**. 1985. Altered fidelity of mitotic chromosome transmission in cell cycle mutants of *S. cerevisiae*. *Genetics* **110**: 381–95.
2. **Sunkel CE**, **Glover DM**. 1988. polo, a mitotic mutant of *Drosophila* displaying abnormal spindle poles. *J Cell Sci* **89** (Pt 1): 25–38.
3. **Wood JS**, **Hartwell LH**. 1982. A dependent pathway of gene functions leading to chromosome segregation in *Saccharomyces cerevisiae*. *J Cell Biol* **94**: 718–26.
4. **Kitada K**, **Johnson AL**, **Johnston LH**, **Sugino A**. 1993. A multicopy suppressor gene of the *Saccharomyces cerevisiae* G1 cell cycle mutant gene dbf4 encodes a protein kinase and is identified as CDC5. *Mol Cell Biol* **13**: 4445–57.

5. **Llamazares S**, **Moreira A**, **Tavares A**, **Girdham C**, et al. 1991. polo encodes a protein kinase homolog required for mitosis in *Drosophila*. *Genes Dev* **5**: 2153–65.
6. **Abrieu A**, **Brassac T**, **Galas S**, **Fisher D**, et al. 1998. The Polo-like kinase Plx1 is a component of the MPF amplification loop at the G2/M-phase transition of the cell cycle in *Xenopus* eggs. *J Cell Sci* **111**(Pt 12): 1751–7.
7. **Clay FJ**, **McEwen SJ**, **Bertoncello I**, **Wilks AF**, et al. 1993. Identification and cloning of a protein kinase-encoding mouse gene, Plk, related to the polo gene of *Drosophila*. *Proc Natl Acad Sci U S A* **90**: 4882–6.
8. **Golsteyn RM**, **Schultz SJ**, **Bartek J**, **Ziemiecki A**, et al. 1994. Cell cycle analysis and chromosomal localization of human Plk1, a putative homologue of the mitotic kinases *Drosophila* polo and *Saccharomyces cerevisiae* Cdc5. *J Cell Sci* **107**(Pt 6): 1509–17.
9. **Golsteyn RM**, **Mundt KE**, **Fry AM**, **Nigg EA**. 1995. Cell cycle regulation of the activity and subcellular localization of Plk1, a human protein kinase implicated in mitotic spindle function. *J Cell Biol* **129**: 1617–28.
10. **Barr FA**, **Sillje HH**, **Nigg EA**. 2004. Polo-like kinases and the orchestration of cell division. *Nat Rev Mol Cell Biol* **5**: 429–40.
11. **de Carcer G**, **Escobar B**, **Higuero AM**, **Garcia L**, et al. Plk5, a polo box domain-only protein with specific roles in neuron differentiation and glioblastoma suppression. *Mol Cell Biol* 31: 1225–39.
12. **de Carcer G**, **Manning G**, **Malumbres M**. From Plk1 to Plk5: functional evolution of polo-like kinases. *Cell Cycle* **10**: 2255–62.
13. **Lane HA**, **Nigg EA**. 1996. Antibody microinjection reveals an essential role for human polo-like kinase 1 (Plk1) in the functional maturation of mitotic centrosomes. *J Cell Biol* **135**: 1701–13.
14. **Tang D**, **Mar K**, **Warren G**, **Wang Y**. 2008. Molecular mechanism of mitotic Golgi disassembly and reassembly revealed by a defined reconstitution assay. *J Biol Chem* **283**: 6085–94.
15. **Wang Y**, **Satoh A**, **Warren G**. 2005. Mapping the functional domains of the Golgi stacking factor GRASP65. *J Biol Chem* **280**: 4921–8.
16. **Preisinger C**, **Korner R**, **Wind M**, **Lehmann WD**, et al. 2005. Plk1 docking to GRASP65 phosphorylated by Cdk1 suggests a mechanism for Golgi checkpoint signalling. *EMBO J* **24**: 753–65.
17. **Tang D**, **Yuan H**, **Vielemeyer O**, **Perez F**, et al. Sequential phosphorylation of GRASP65 during mitotic Golgi disassembly. *Biol Open* **1**: 1204–14.
18. **Budde PP**, **Kumagai A**, **Dunphy WG**, **Heald R**. 2001. Regulation of Op18 during spindle assembly in *Xenopus* egg extracts. *J Cell Biol* **153**: 149–58.
19. **van Vugt MA**, **van de Weerdt BC**, **Vader G**, **Janssen H**, et al. 2004. Polo-like kinase-1 is required for bipolar spindle formation but is dispensable for anaphase promoting complex/Cdc20 activation and initiation of cytokinesis. *J Biol Chem* **279**: 36841–54.
20. **Sumara I**, **Gimenez-Abian JF**, **Gerlich D**, **Hirota T**, et al. 2004. Roles of polo-like kinase 1 in the assembly of functional mitotic spindles. *Curr Biol* **14**: 1712–22.
21. **Maia AR**, **Garcia Z**, **Kabeche L**, **Barisic M**, et al. Cdk1 and Plk1 mediate a CLASP2 phospho-switch that stabilizes kinetochore-microtubule attachments. *J Cell Biol* **199**: 285–301.
22. **Godinho S**, **Tavares AA**. 2008. A role for *Drosophila* Polo protein in chromosome resolution and segregation during mitosis. *Cell Cycle* **7**: 2529–34.
23. **Kang YH**, **Park JE**, **Yu LR**, **Soung NK**, et al. 2006. Self-regulated Plk1 recruitment to kinetochores by the Plk1-PBIP1 interaction is critical for proper chromosome segregation. *Mol Cell* **24**: 409–22.
24. **Burkard ME**, **Maciejowski J**, **Rodriguez-Bravo V**, **Repka M**, et al. 2009. Plk1 self-organization and priming phosphorylation of HsCYK-4 at the spindle midzone regulate the onset of division in human cells. *PLoS Biol* **7**: e1000111.
25. **Burkard ME**, **Randall CL**, **Larochelle S**, **Zhang C**, et al. 2007. Chemical genetics reveals the requirement for Polo-like kinase 1 activity in positioning RhoA and triggering cytokinesis in human cells. *Proc Natl Acad Sci U S A* **104**: 4383–8.
26. **Neef R**, **Preisinger C**, **Sutcliffe J**, **Kopajtich R**, et al. 2003. Phosphorylation of mitotic kinesin-like protein 2 by polo-like kinase 1 is required for cytokinesis. *J Cell Biol* **162**: 863–75.
27. **Petronczki M**, **Glotzer M**, **Kraut N**, **Peters JM**. 2007. Polo-like kinase 1 triggers the initiation of cytokinesis in human cells by promoting recruitment of the RhoGEF Ect2 to the central spindle. *Dev Cell* **12**: 713–25.
28. **Qian YW**, **Erikson E**, **Maller JL**. 1999. Mitotic effects of a constitutively active mutant of the *Xenopus* polo-like kinase Plx1. *Mol Cell Biol* **19**: 8625–32.
29. **Seong YS**, **Kamijo K**, **Lee JS**, **Fernandez E**, et al. 2002. A spindle checkpoint arrest and a cytokinesis failure by the dominant-negative polo-box domain of Plk1 in U-2 OS cells. *J Biol Chem* **277**: 32282–93.
30. **Wolfe BA**, **Takaki T**, **Petronczki M**, **Glotzer M**. 2009. Polo-like kinase 1 directs assembly of the HsCyk-4 RhoGAP/Ect2 RhoGEF complex to initiate cleavage furrow formation. *PLoS Biol* **7**: e1000110.
31. **Bibi N**, **Parveen Z**, **Rashid S**. Identification of potential Plk1 targets in a cell-cycle specific proteome through structural dynamics of kinase and Polo box-mediated interactions. *PLoS One* **8**: e70843.
32. **Lowery DM**, **Mohammad DH**, **Elia AE**, **Yaffe MB**. 2004. The Polo-box domain: a molecular integrator of mitotic kinase cascades and Polo-like kinase function. *Cell Cycle* **3**: 128–31.
33. **Park JE**, **Soung NK**, **Johmura Y**, **Kang YH**, et al. Polo-box domain: a versatile mediator of polo-like kinase function. *Cell Mol Life Sci* **67**: 1957–70.
34. **Cheng KY**, **Lowe ED**, **Sinclair J**, **Nigg EA**, et al. 2003. The crystal structure of the human polo-like kinase-1 polo box domain and its phospho-peptide complex. *EMBO J* **22**: 5757–68.
35. **Elia AE**, **Rellos P**, **Haire LF**, **Chao JW**, et al. 2003. The molecular basis for phosphodependent substrate targeting and regulation of Plks by the Polo-box domain. *Cell* **115**: 83–95.
36. **Garcia-Alvarez B**, **de Carcer G**, **Ibanez S**, **Bragado-Nilsson E**, et al. 2007. Molecular and structural basis of polo-like kinase 1 substrate recognition: implications in centrosomal localization. *Proc Natl Acad Sci U S A* **104**: 3107–12.
37. **Elia AE**, **Cantley LC**, **Yaffe MB**. 2003. Proteomic screen finds pSer/pThr-binding domain localizing Plk1 to mitotic substrates. *Science* **299**: 1228–31.
38. **Archambault V**, **D'Avino PP**, **Deery MJ**, **Lilley KS**, et al. 2008. Sequestration of Polo kinase to microtubules by phosphopriming-independent binding to Map205 is relieved by phosphorylation at a CDK site in mitosis. *Genes Dev* **22**: 2707–20.
39. **Liu X**, **Erikson RL**. 2002. Activation of Cdc2/cyclin B and inhibition of centrosome amplification in cells depleted of Plk1 by siRNA. *Proc Natl Acad Sci U S A* **99**: 8672–6.
40. **Liu X**, **Erikson RL**. 2003. Polo-like kinase (Plk)1 depletion induces apoptosis in cancer cells. *Proc Natl Acad Sci U S A* **100**: 5789–94.
41. **Lenart P**, **Petronczki M**, **Steegmaier M**, **Di Fiore B**, et al. 2007. The small-molecule inhibitor BI 2536 reveals novel insights into mitotic roles of polo-like kinase 1. *Curr Biol* **17**: 304–15.
42. **Carmena M**, **Riparbelli MG**, **Minestrini G**, **Tavares AM**, et al. 1998. *Drosophila* polo kinase is required for cytokinesis. *J Cell Biol* **143**: 659–71.
43. **Herrmann S**, **Amorim I**, **Sunkel CE**. 1998. The POLO kinase is required at multiple stages during spermatogenesis in *Drosophila melanogaster*. *Chromosoma* **107**: 440–51.
44. **Lee KS**, **Park JE**, **Asano S**, **Park CJ**. 2005. Yeast polo-like kinases: functionally conserved multitask mitotic regulators. *Oncogene* **24**: 217–29.
45. **Winkles JA**, **Alberts GF**. 2005. Differential regulation of polo-like kinase 1, 2, 3, and 4 gene expression in mammalian cells and tissues. *Oncogene* **24**: 260–6.
46. **Yuan J**, **Horlin A**, **Hock B**, **Stutte HJ**, et al. 1997. Polo-like kinase, a novel marker for cellular proliferation. *Am J Pathol* **150**: 1165–72.
47. **Takai N**, **Hamanaka R**, **Yoshimatsu J**, **Miyakawa I**. 2005. Polo-like kinases (Plks) and cancer. *Oncogene* **24**: 287–91.
48. **Eckerdt F**, **Yuan J**, **Strebhardt K**. 2005. Polo-like kinases and oncogenesis. *Oncogene* **24**: 267–76.
49. **Strebhardt K**, **Ullrich A**. 2006. Targeting polo-like kinase 1 for cancer therapy. *Nat Rev Cancer* **6**: 321–30.
50. **de Carcer G**, **Perez de Castro I**, **Malumbres M**. 2007. Targeting cell cycle kinases for cancer therapy. *Curr Med Chem* **14**: 969–85.
51. **Chopra P**, **Sethi G**, **Dastidar SG**, **Ray A**. Polo-like kinase inhibitors: an emerging opportunity for cancer therapeutics. *Expert Opin Investig Drugs* **19**: 27–43.
52. **Strebhardt K**. Multifaceted polo-like kinases: drug targets and antitargets for cancer therapy. *Nat Rev Drug Discov* **9**: 643–60.
53. **Lu LY**, **Wood JL**, **Minter-Dykhouse K**, **Ye L**, et al. 2008. Polo-like kinase 1 is essential for early embryonic development and tumor suppression. *Mol Cell Biol* **28**: 6870–6.
54. **Raab M**, **Kappel S**, **Kramer A**, **Sanhaji M**, et al. 2011. Toxicity modelling of Plk1-targeted therapies in genetically engineered mice and cultured primary mammalian cells. *Nat Commun* **2**: 395.
55. **Rodriguez CI**, **Buchholz F**, **Galloway J**, **Sequerra R**, et al. 2000. High-efficiency deleter mice show that FLPe is an alternative to Cre-loxP. *Nat Genet* **25**: 139–40.
56. **Qian YW**, **Erikson E**, **Li C**, **Maller JL**. 1998. Activated polo-like kinase Plx1 is required at multiple points during mitosis in *Xenopus laevis*. *Mol Cell Biol* **18**: 4262–71.
57. **Lindqvist A**, **Rodriguez-Bravo V**, **Medema RH**. 2009. The decision to enter mitosis: feedback and redundancy in the mitotic entry network. *J Cell Biol* **185**: 193–202.
58. **van Vugt MA**, **Bras A**, **Medema RH**. 2004. Polo-like kinase-1 controls recovery from a G2 DNA damage-induced arrest in mammalian cells. *Mol Cell* **15**: 799–811.
59. **Lera RF**, **Burkard ME**. 2012. High mitotic activity of Polo-like kinase 1 is required for chromosome segregation and genomic integrity in human epithelial cells. *J Biol Chem* **287**: 42812–25.
60. **Oshimori N**, **Ohsugi M**, **Yamamoto T**. 2006. The Plk1 target Kizuna stabilizes mitotic centrosomes to ensure spindle bipolarity. *Nat Cell Biol* **8**: 1095–101.
61. **De Luca M**, **Lavia P**, **Guarguaglini G**. 2006. A functional interplay between Aurora-A, Plk1 and TPX2 at spindle poles: Plk1 controls centrosomal localization of Aurora-A and TPX2 spindle association. *Cell Cycle* **5**: 296–303.
62. **Baran V**, **Solc P**, **Kovarikova V**, **Rehak P**, et al. 2013. Polo-like kinase 1 is essential for the first mitotic division in the mouse embryo. *Mol Reprod Dev* **80**: 522–34.
63. **Solc P**, **Kitajima TS**, **Yoshida S**, **Brzakova A**, et al. 2015. Multiple requirements of PLK1 during mouse oocyte maturation. *PLoS One* **10**: e0116783.
64. **Garcia-Higuera I**, **Manchado E**, **Dubus P**, **Canamero M**, et al. 2008. Genomic stability and tumour suppression by the APC/C cofactor Cdh1. *Nat Cell Biol* **10**: 802–11.